Effective Color Components for Pupil Diameter Measurement of Brown Eye Using a Visible-light Camera

Kazuki Tachi
Graduate School of Engineering,
Toyama Prefectural University
Toyama, JAPAN
Email: tachi@neu.pu-toyama.ac.jp,

Hironobu Takano
Graduate School of Engineering,
Toyama Prefectural University
Toyama, JAPAN
Email: takano@pu-toyama.ac.jp

***Abstract*—The pupil diameter variation are used for various intelligent system. The measurement of pupil diameter is generally performed using eye images taken with a near-infrared camera. However, the near-infrared camera is not mounted on a general PC or mobile devices. Therefore, if the pupil diameter can be measured using a visible-light camera mounted on a general PC or mobile devices, the system using pupil diameter variation can be generalized. In this paper, we investigate the effective color components for pupil detection using the visible-light camera under visible-light conditions. From the experimental results, the effective color components for pupil detection and pupil diameter measurement are R in RGB color space and H in HSV color space. In addition, as a result of measuring the pupil diameter with R and H color components, the accuracy of the visible-light camera is almost same as that of the near-infrared camera.**

***Index Terms*—Pupil detection, Visible-light camera, Color space**

I. Introduction

The pupil diameter is varied by the amount of incident light. However, the factor of pupil diameter variation is not only control of incident light but also control by the autonomic nervous system, e.g. emotion, fatigue, interest, and attention. The various systems have been developed using pupil diameter variation due to this emotional change [1]–[3]. For example, the recommendation system in which the pupil diameter variation estimates human's interest is developed [4]. The pupillary reaction is time series variation of pupil diameter. Normally, pupil diameter is measured by using eye image captured with a near-infrared camera and performing image processing. The near-infrared illumination is also required to capture the pupil. However, the near-infrared camera and illumination required for measuring the pupil diameter is not mounted on a general PC or mobile devices. The general PC and mobile devices equip visible-light cameras. If the pupil diameter can be measured using a visible-light camera, various recommendation systems can be developed by generalization. For example, user's eye tracking, autonomic activity measurement, and emotion estimation would be performed by a PC or mobile devices.

The color of the most pupil in the world is brown. The brown pupil taken with a visible-light camera is shown in Fig.1. The purpose of this study is to generalize the pupil diameter measurement system for brown eyes under visible-light conditions. As shown in Fig.1, the brown pupil captured with a visible-light camera includes corneal reflection. Therefore, it is difficult to distinguish the pupil portion from the iris region. The pupil detection method using the edge detection by the Canny operator and the circular Hough transform has been proposed [5]. In this method, first, a color eye image captured with a visible-light camera is converted to a gray-scale image. After that, the pupil diameter in the gray-scale image is measured by using edge detection with Canny operator and Hough transform. Here, the gray-scale conversion requires the color component which enables to discriminate the pupil portion from iris region. In this paper, we investigate the effective color component for pupil detection under the visible-light condition. In the evaluation experiment, we used the eye images which are obtained by capturing Japanese brown eyes.

This paper organized as follows. Section 2 shows related works. Section 3 presents the pupil detection method. Section 4 describes the experimental method to investigate the effective color component for pupil detection under the visible-light environment. Section 5 shows the experimental results, and Section 6 shows discussion. Finally, we describe our conclusions in Section 7.

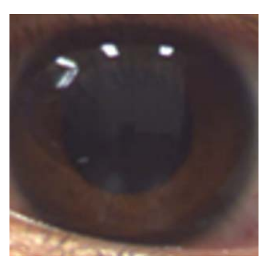

Fig. 1. Brown pupil taken with a visible-light camera

2577-1655/18/$31.00 ©2018 IEEE
DOI 10.1109/SMC.2018.00152

II. Related Works

In this section, we introduce previous researches on object detection focusing on color components. In the robot application, in order to recognize an object in real time, Caleiro et al. studied to accurately detect color-coded objects with specific colors[6]. In this research, various color spaces which were four color spaces of RGB, HLS, HSV, and IHLS were used for the object detection. The visible-light camera is used for capturing objects. As a result, more accurate detection can be performed by adjusting the white balance in the HSV color space.

In our study, the pupil and iris regions are distinguished by using color component. As a research for classification of two regions, Ershad et al. proposed a skin detection method using color components and image retrieval technology[7]. By this method, it is possible to distinguish between skin and non-skin regions. In addition, this study is not only skin detection but also classification of three types of skin. First, the skin detection method calculates the skin feature vectors in the RGB color space. Next, the portion similar to the skin feature vectors is searched in the input image. Finally, if the degree of similarity between the searched part and the skin is equal or greater than a certain value, it is determined as the skin. The detection accuracy is improved by the image tiling which prevents the overlooked detection of skin region. As a result, skin detection can be performed with an accuracy of 93%.

There are various studies focusing on color components except above studies [8]–[13]. It is possible to detect objects using various color spaces. However, it is unclear which color component is more suitable for pupil detection. In the pupil detection, the corneal reflection appears in the captured eye image as shown in Fig.1. In this paper, we investigate the effective color components for pupil detection under visible-light conditions.

III. Pupil Detection Method

The flowchart of pupil detection method is shown in Fig.2. First, the iris portion is extracted from the eye image. As the method of the iris portion extraction, we used the Canny filter. First, a color eye image is converted to a gray-scale image using only blue component. This gray-scale conversion increases the edge intensity of the iris contour. Next, the iris edges are detected using the Canny filter. Then, we performed circle detection by the Hough transformation with the detected iris edge points. As a result, the iris portion can be detected. By extracting the iris portion, the pupil can be detected more accurately. The image obtained by extracting the iris portion is shown in Fig.3(a).

Next, we used gray-scale conversion with various color components in the iris portion image. The color components used for the gray-scale conversion are RGB and HSV. The R, G, and B mean red, green and blue color components, respectively. The H, S and V mean Hue indicating the difference in color, Saturation indicating chroma, and Value indicating brightness, respectively. The H, S, and V are obtained by (3) – (5). After that, the histogram equalization and noise reduction are performed with each gray-scale image. Figures3(b), (c), and (d) show the image obtained by the gray-scale conversion with the R component, the image obtained by the histogram equalization, and the image after noise reduction, respectively. Then, edge detection by the Canny filter is performed to the image of Fig.3(d). Finally, the circle is detected by Hough transformation with the detected edge points. The detected circle is estimated as the pupil contour.

When the Canny filter for edge detection is used, it is necessary to decide the threshold of the weak edge and strong edge. The threshold of weak edge is half the value of strong edge. The threshold value of strong edge is decided as follows. First, pupil detection is performed by changing the threshold value from 10 to 70 every 5. Next, the detection results of 10 to 70 are obtained. Finally, the threshold with the highest detection rate is taken as the threshold of strong edge. As a result, the thresholds of strong edge for R, G, B, H, S, and V were decided as 50, 10, 10, 10, 30, and 10, respectively.

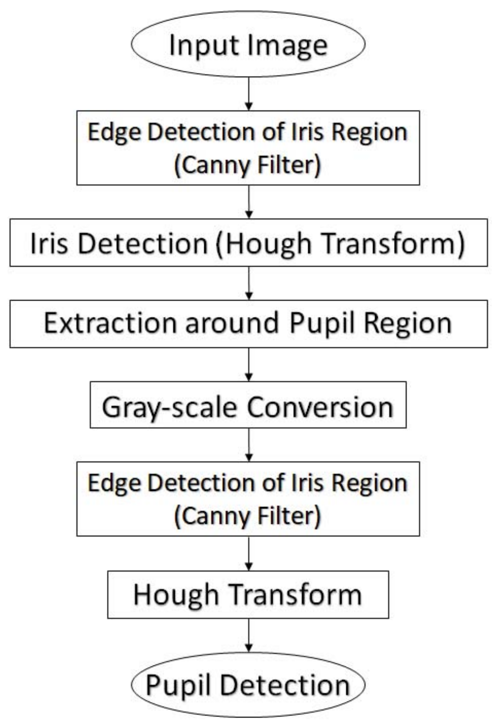

Fig. 2. Flowchart of pupil detection

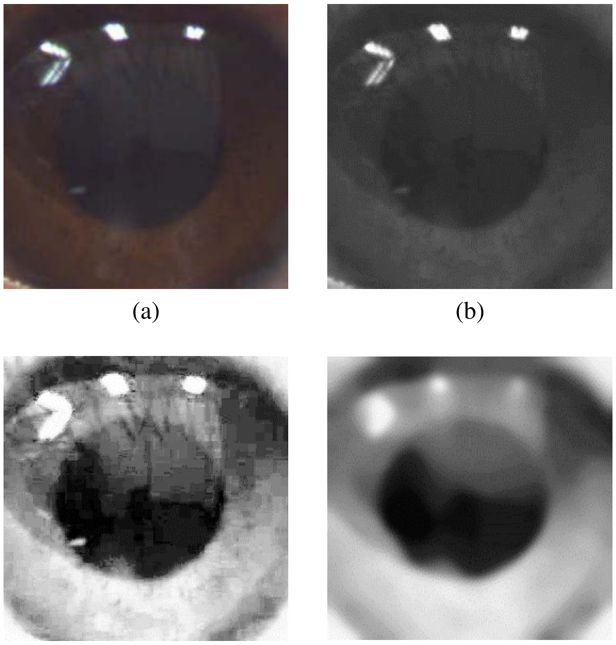

(a) (b) (c) (d)

Fig. 3. Image after each processing

$$l_{max} = max\{R, G, B\} \tag{1}$$

$$l_{min} = min\{R, G, B\} \tag{2}$$

$$H = \begin{cases} \dfrac{(G-B)}{l_{max}-l_{min}} \times 60 & (l_{max} = R) \\[2ex] \dfrac{(B-R)}{l_{max}-l_{min}} \times 60 + 120 & (l_{max} = G) \\[2ex] \dfrac{(R-G)}{l_{max}-l_{min}} \times 60 + 240 & (l_{max} = B) \end{cases} \tag{3}$$

$$S = \begin{cases} \dfrac{l_{max}}{(l_{max}-l_{min})} & (if\ V \neq 0) \\ 0 & (otherwise) \end{cases} \tag{4}$$

$$V = l_{max} \tag{5}$$

IV. Experimental Method

The pupil was detected by the method described in Section 3. In this section, we describe the brown eye image acquisition method and evaluation method of experiments. These experiments were approved by the Ethics Committee of Toyama Prefectural University. Written informed consent was obtained from each participant.

A. Capturing Method

The eye images were taken using a visible-light camera (Argo Lw115-IO). The subjects were 10 students (8 males and 4 females) from 21 to 24 years old. We obtained 47 eye images in total. The eye image captured with the visible-light camera is shown in Fig.4. The size of eye image is 1280 × 1080 [pixels]. The capturing environment is as follows. Capturing was done indoors. White fluorescent lamps are installed in the room. When the eye image was captured, light other than white fluorescent lighting was prevented from entering around subject's eye. Also, the subject's head was fixed by using the chin support device during capturing his/her eye.

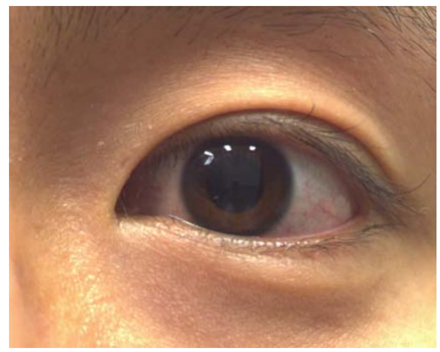

Fig. 4. Eye image captured with the visible-light camera

B. Evaluation Method

For the evaluation of pupil detection result, the pupil center position and the pupil diameter are measured. The evaluation is performed by comparing the measurement results of each color component and their true values. First, in order to evaluate pupil center position and pupil diameter, each true value is measured. The method of measuring the true value is shown as follows. First, the circle is fitted to the pupil contour of the input image manually. Next, the center coordinates and diameter of the fitted circle are obtained as the true value of pupil center position and diameter, respectively.

For the evaluation, the Euclidean distance between the measured pupil center coordinates and its true coordinates, and the difference between measured pupil diameter and its true value are calculated. The Euclidean distance and difference of pupil diameter are calculated by (6) and (7), respectively. In (6), x_{cc} and y_{cc} are x and y position values of the measured pupil center position, respectively. The x_{ac} and y_{ac} are true values, which are the x and y position of the pupil center, respectively. E_c [pixel] means the Euclidean distance between the measured and true values of pupil center position. In (7), D_{mv} is measured value of the pupil diameter, and D_{ac} is true value of the pupil diameter. $|E_{pd}|$ [pixel] means the absolute difference between D_{mv} and D_{ac}.

The units of E_c and $|E_{pd}|$ in pixel are changed into the unit in millimeter as follow. The length of 1 millimeter in an image is measured as the unit of pixels by capturing a ruler with the camera used for the experiment. As a result of this measurement, the length per 1 [mm] was 34 [pixels]. Therefore, we evaluate the pupil detection accuracy with comparison result obtained in the unit of millimeter.

$$E_c = \sqrt{(x_{cc} - x_{ac})^2 + (y_{cc} - y_{ac})^2} \tag{6}$$

$$|E_{pd}| = D_{mv} - D_{ac} \tag{7}$$

V. Experimental Results

As described in Section 3, the color components for gray-scale conversion are R, G, B, H, S, and V. Therefore, pupil detection results of six color components were obtained.

The averages and standard deviations for the difference of pupil center position are shown in Fig.5. The averages and standard deviations for the absolute difference of pupil diameter are shown in Fig.6. In Figs.5 and 6, the vertical axes show the E_c [mm] and $|E_{pd}|$ [mm] and the horizontal axes show the color components. In addition, in order to investigate the significant difference of E_c and $|E_{pd}|$ obtained with each color component, the Tukey's multiple comparison test was performed. The results of Tukey's multiple comparison test are shown in Tables I and II. In Tukey's multiple comparison test, the color components with significant difference in the six kinds of color components is indicated by asterisk. In Tables I and II, the numbers of asterisk indicate their respective significance levels.

In Fig.5, the average of E_c obtained with the R color component was the smallest, and the color component having the largest E_c was the B component. From overall comparison, the E_c for the R, H, and V components were small, and E_c for the G, B, and S components were relatively large. In Fig.6, the average of $|E_{pd}|$ obtained with the R color component was the smallest, and the color component having the largest $|E_{pd}|$ was the B component. From overall comparison, the $|E_{pd}|$ for the R, H, S and V components were relatively small, and the $|E_{pd}|$ for the G and B components were large. From comprehensive comparison result, the R component has the smallest difference of both the pupil center position and the pupil diameter. The absolute difference between the pupil center position and the pupil diameter of the H component is also small. These results indicate that the R and H components are effective to separate the pupil region from the brown iris region under the visible-light condition. Figures 7 (a) and (b) show gray-scale images converted with R and H components, and Figures 7 (c) and (d) show gray-scale images converted with G and B components. In Fig.7, it is easy to confirm the boundary between the iris and pupil in effective color components (R and H). On the other hand, the boundary between the iris and pupil is unclear in the image converted with G or B components.

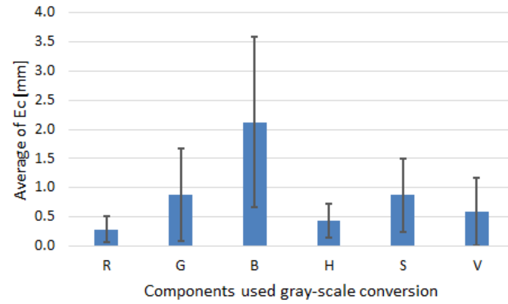

Fig. 5. Average and standard deviation for the difference of pupil center position

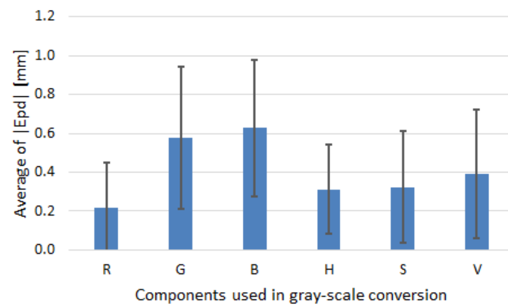

Fig. 6. Average and standard deviation for absolute difference of pupil diameter

TABLE I
Result of Tukey's multiple comparison test for E_c

($*$=p<0.05, $**$=p<0.01, $***$=p<0.001)

	R	G	B	H	S	V
R	—	**	***		**	
G	—	—	***			
B	—	—	—	***	***	***
H	—	—	—	—		
S	—	—	—	—	—	
V	—	—	—	—	—	—

TABLE II
Result of Tukey's multiple comparison test for $|E_{pd}|$

($*$=p<0.05, $**$=p<0.01, $***$=p<0.001)

	R	G	B	H	S	V
R	—	***	***			
G	—	—		**	**	
B	—	—	—	***	***	**
H	—	—	—	—		
S	—	—	—	—	—	
V	—	—	—	—	—	—

VI. Discussion

In this section, we describe the findings obtained from the experimental results and the processing time of the pupil detection method.

A. Experimental results

Experimental results showed that the R and H components are effective for separating the pupil region. Also, it was shown that the G, B, S and V color components are not suitable for separating the pupil region. The edge detection results of the gray-scale images in Fig.7 by the Canny filter are shown in Fig.8. In Fig.8, the edge detection results with R and H components roughly show the contour of the pupil portion, but the pupil contour cannot be identified in the edge detection results with G and B components. Therefore, it is considered that there are effective or undesirable color components for separating the pupil position.

B. Processing time

The purpose of this study is to generalize the system using pupil variation. Therefore, it is necessary to measure the pupil diameter in real-time. From the experimental result, the average and standard deviation of the processing time per an image was 406$\pm$187[ms]. In this system, it takes a long time to detect the pupil contour by Hough transformation. Therefore, the contour extraction method with low computational cost should be adopted.

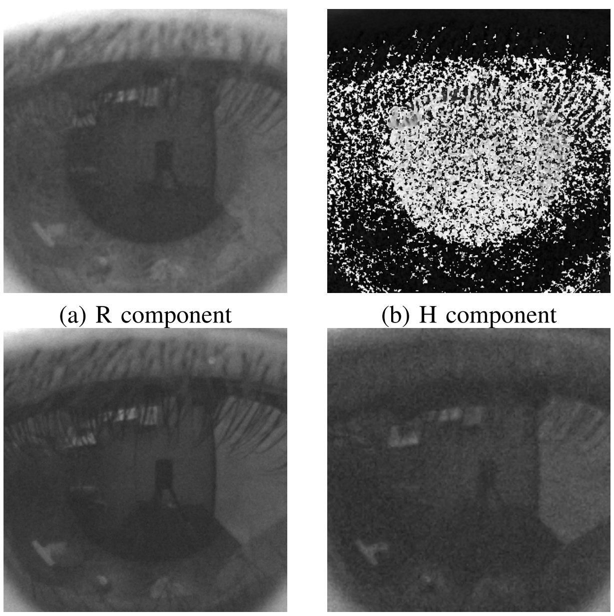

(a) R component (b) H component

(c) G component (d) B component

Fig. 7. Image after each processing

VII. Conclusions

In this study, we investigate the effective color components for pupil detection under the visible-light condition. The six color components (RGB and HSV) were used in the experiment. In order to detect the pupil with each color component, the input image was converted to the gray-scale image with each color component. In the experiment, pupil detection using Canny filter and Hough transform was performed. As results of detecting the pupil with each color component, R and H color components were effective. In addition, it was suggested that pupil can be detected even with a visible-light camera.

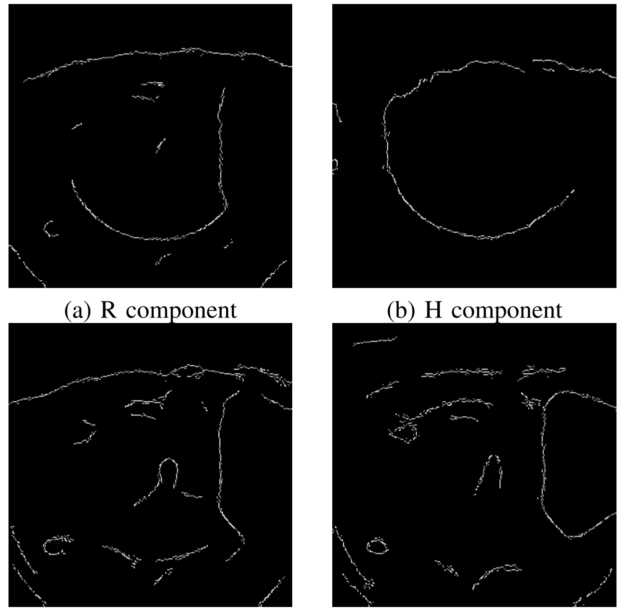

(a) R component (b) H component

(c) G component (d) B component

Fig. 8. The results of edge detection by the Canny filter

In future works, it is necessary to conduct pupil detection experiment for various iris colors. The iris color of most Asians is brown. However, in other areas, there are other color irises such as blue and green. The R and H components were effective for brown iris, but it is unclear whether the R and H color components are effective for other iris colors or not. Therefore, it is necessary to develop a pupil detection method selecting the color component of gray-scale conversion appropriate for iris color. We also plan to develop a pupil detection method combining multiple color components.

References

[1] A. Babiker, I. Faye, K. Prehn, and A. Malik, “Machine learning to differentiate between positive and negative emotions using pupil diameter,” Frontiers in Psychology, Vol.6, 2015.

[2] M. Iwata and Y. Ebihara, “PupilMouse supported by head pose detection,” Proc. VECIMS2008, pp.178–183, 2008.

[3] N. Y. Sokhour, M. Sugano, P. Sriprasertsuk, and W. Kameyama, “A consideration on comic reader’s behavior using gaze path and pupil size,” IPSJ SIG Technical Report, Vol.2012-AVM-79, No.26, pp.139–144, 2012.

[4] S. Ito, Y. kajiwara, F. Harada, and H. Shimakawa, “Touch gesture and pupil reaction on mobile terminal to find occurrences of interested items in web browsing,” Scientific Academic Publishing, International Journal of Web Engineering, Vol.5, No.1, pp.1–9, 2016.

[5] M. Soltany and H. R. Pourreza, “Fast and accurate pupil positioning algorithm using circular hough transform and gray projection,” Proc. CSIT, Vol.5, pp.556–561, 2011.

[6] P. M. R. Caleiro, A. J. R. Neves, and A. J. Pinho, “Color-spaces and color segmentation for real-time object recognition in robotic applications,” REVISTA DO DETUA, Vol.4, No.8, 2007.

[7] S. F. Ershad, M. Saberi, and F. Tajeripour, "An innovative skin detection approach using color based image retrieval technique," The International Journal of Multimedia & Its Applications (IJMA), Vol.4, No.3, pp.57–65, 2012.
[8] V. Goel, S. Singhal, T. Jain, and S. Kole, "Specific color detection in images using RGB modelling in MATLAB," International Journal of Computer Applications, Vol.161, No.8, pp.38–42, 2017.
[9] K. B. Shaika, P. Ganesan, V. Kalist, B. S. Sathish, and J. M. M. Jenithab, "Comparative study of skin color detection and segmentation in HSV and YCbCr color space," Procedia Computer Science, Vol.57, pp.41–48, 2015.
[10] P. He, Y. Wan, P. Jiang, and J. Qin, "Automatic houses detection with color aerial images based on image segmentation," Journal of the International Society of Sports Nutrition, pp.1927–1932, 2014.
[11] P. J. Navarro, D. Alonso, and K. Stathis, "Automatic detection of microaneurysms in diabetic retinopathy fundus images using the L*a*b color space," Journal of the Optical Society of America A, Vol.33, pp.74–83, 2016.
[12] W. Shi and J. Li, "Shadow detection in color aerial images based on HSI space and color attenuation relationship," EURASIP Journal on Advances in Signal Processing, 2012.
[13] P. S. Hiremath and A. Danti, "Detection of multiple faces in an image using skin color information and lines-of-separability face mode," International Journal of Pattern Recognition and Artificial Intelligence, Vol.20, pp.20–39, 2006.